Kinetic Studies of CO_2 Insertion into Metal-Element σ-Bonds

Nilay Hazari*

The Department of Chemistry, Yale University, P. O. Box 208107, New Haven, Connecticut, 06520, USA. E-mail: nilay.hazari@yale.edu

Graphic for Conspectus

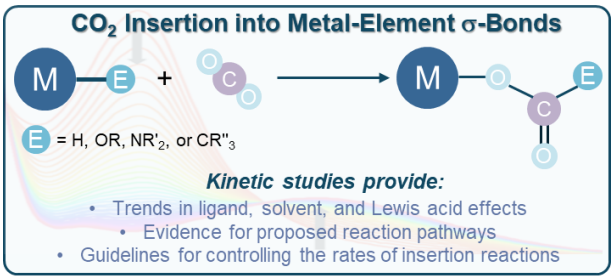

Conspectus

Despite the plethora of metal catalyzed reactions for CO_2 utilization that have been developed in academic laboratories, practical systems remain elusive. The understanding of the elementary steps in catalysis is a proven method to improve catalytic performance. In many catalytic cycles for CO_2 utilization, the insertion of CO_2 into a metal-element σ-bond, such as hydrides, alkyls, amides, or hydroxides, is a crucial step. However, despite the many demonstrations of CO_2 insertion, there are a paucity of kinetic studies, and information about reaction mechanism has been predominantly elucidated from computational investigations. In this *Account*, kinetic studies on CO_2 insertion into late transition metal-element σ-bonds performed by my group are summarized, along with their implications for catalysis.

A common pathway for CO_2 insertion into a metal hydride involves a two-step mechanism. The first step is nucleophilic attack on CO_2 by the hydride to generate an H-bound formate, followed by rearrangement to form an O-bound formate product. Kinetic studies on systems in which both the first and second steps are proposed to be rate-determining, known as innersphere and outersphere processes, respectively, show that insertion rates increase as: (i) the ligand *trans* to the hydride becomes a stronger donor, (ii) the ancillary ligand becomes more electron-donating, and (iii) the Dimroth-Reichart parameter of the solvent increases. However, the magnitude of these effects is generally smaller for innersphere processes because there is less build-up of charge in the key transition state. For similar reasons, the presence of Lewis acids only increases the rate of outersphere processes. These results suggest it may be possible to experimentally differentiate between inner and outersphere processes.

The insertion of CO_2 into a metal alkyl bond results in the formation of a C–C bond, which is important for the generation of fuels from CO_2. The presence of a strong donor ligand *trans* to the alkyl group is critical for kinetically promoting insertion. Further, the nucleophilicity of the alkyl ligand directly impacts the rate of CO_2 insertion via an S_E2 mechanism, as does the steric bulk of the complex, and the reaction solvent. In contrast, to the relatively slow rates of insertion observed for metal alkyls, CO_2 insertion is rapid for metal hydroxides and amides. Although

kinetics trends could be determined for hydroxides, reactions with amides are too fast for quantitative studies.

Overall, the rates of insertion correlate with the nucleophilicity of the element in the metal-element σ-bond, so amide > hydroxide > hydride > alkyl. Due to the related pathways for insertion, similar trends in ligand and solvent effects are observed for insertion into different metal-element σ-bonds. Thus, the same strategies can be used to control the rates of insertion across systems. Differences in the magnitude of solvent and ligand effects are caused by variation in the amount of charge build-up on the metal in the rate-determining transition state. Likely, given that CO_2 is related to organic molecules such as aldehydes, ketones and amides, the results described in this *Account* are general to a wider range of substrates.

Key References

- Schmeier, T. J.; Dobereiner, G. E.; Crabtree, R. H.; Hazari, N. 'Secondary Coordination Sphere Interactions Facilitate the Insertion Step in an Iridium(III) CO_2 Reduction Catalyst.' *J. Am. Chem. Soc.* **2011**, *133*, 9274-9277.[1] *A non-quantitative example of ligand effects on CO_2 insertion into a series of Ir hydrides.*
- Heimann, J. E.; Bernskoetter, W. H.; Hazari, N.; Mayer, J. M. 'Acceleration of CO_2 Insertion into Metal Hydrides: Ligand, Lewis Acid, and Solvent Effects on Reaction Kinetics.' *Chem. Sci.* **2018**, *9*, 6629-6638.[2] *A quantitative comparison of differences in the rates of CO_2 insertion between Ni and Ir hydrides as factors such as solvent and presence of Lewis acid are varied.*
- Heimann, J. E.; Bernskoetter, W. H.; Hazari, N. 'Understanding the Individual and Combined Effects of Solvent and Lewis Acid on CO_2 Insertion into a Metal Hydride.' *J. Am. Chem. Soc*. **2019**, *141*, 10520-10529.[3] *The first quantitative study of the impact of different Lewis acids on the rates of CO_2 insertion into a metal hydride that is not impacted by ion-pairing effects.*
- Deziel, A. P.; Espinosa, M. R.; Pavlovic, L.; Charboneau, D. J.; Hazari, N.; Hopmann, K. H.; Mercado, B. Q. 'Ligand and Solvent Effects on CO_2 Insertion into Group 10 Metal Alkyl Bonds.' *Chem. Sci*, **2022**, *13*, 2391-2404.[4] *A rare example of a quantitative study of the rates of CO_2 insertion into a Group 10 alkyl complex.*

Introduction

CO_2 is an attractive target as a chemical feedstock due to its low cost, non-toxic nature, and abundance.[5] There are several chemicals currently industrially prepared from CO_2 such as urea and cyclic carbonates, but only a small fraction of our available CO_2 is used as a feedstock for either commodity or fine chemical synthesis.[5c] The full exploitation of CO_2 as a feedstock is limited by its kinetic and thermodynamic stability, which poses a scientific challenge for developing CO_2-based synthetic routes to more valuable chemicals. Significant progress has been made in solving the kinetic challenges associated with CO_2 conversion through the discovery of catalysts for photo-, electro-, and thermochemical CO_2 reduction into products such as CO, formate, methanol, and acrylic acid.[5] However, only a small number of systems with the potential to be practical have been developed. A well-established strategy to improve catalytic systems is to gain knowledge of reaction mechanisms. Thus, fundamental studies to elucidate the reaction pathways of individual elementary steps in catalytic CO_2 conversion will likely be beneficial.

One of the most promising approaches for the conversion of CO_2 into value-added chemicals is to use transition metal catalysts.[5] CO_2 can bind to many transition metals, and in some cases, coordination of CO_2 weakens the C=O double bonds and facilitates further transformation.[6] However, for thermochemical CO_2 conversion, this strategy often requires the use of highly reactive electrophiles after CO_2 binding and is thus unlikely to lead to practical catalytic reactions. Another method for the activation and subsequent transformation of CO_2 involves the insertion of CO_2 into M–X bonds (for example X = H, OR, NR'$_2$, or CR"$_3$) (Eq 1).[6] CO_2 insertion into late transition metal-element σ-bonds is particularly attractive due to the relative weakness of the M–O bonds that are formed,[6] making cleavage of the M–O bond and further transformation more facile. For example, CO_2 insertion into Ir hydrides is a key step in thermochemical systems for CO_2 hydrogenation to formate.[1,7]

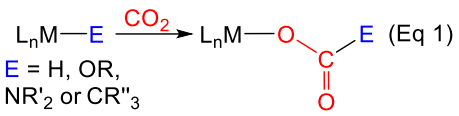

(Eq 1)

There are now many examples of CO_2 insertion into metal-element σ-bonds featuring both transition metal and actinide complexes.[6] Typically, these studies have focused on demonstrating that a complex reacts with CO_2, rather than understanding the mechanism of insertion. Kinetic investigations that provide detailed information on metal, ligand, and solvent effects are relatively rare. Consequently, a large amount of mechanistic information about the pathways for CO_2

insertion has been gained from computational studies, which can often only provide limited information about the role of solvent or common additives in catalysis, such as Lewis Acids, on the rate of the insertion reaction. In this *Account*, I summarize my group's kinetic studies on CO_2 insertion into metal-element σ-bonds focusing predominantly on late transition metal complexes. Connections between trends observed for CO_2 insertion into metal hydrides, alkyls, amides, and hydroxides are drawn and the impact of Lewis Acids and solvent on insertion is described. Throughout the *Account* the connections between our studies on CO_2 insertion and catalytic CO_2 conversion are described.

Carbon Dioxide Insertion into Metal Hydride Bonds

The insertion of CO_2 into a transition metal hydride is a key step in many catalytic transformations involving CO_2.[6] For instance, in electrochemical routes for CO_2 conversion to formate, the insertion of CO_2 into a metal hydride is proposed to be crucial.[8] Similarly, the microscopic reverse reaction – the decarboxylation of a metal formate to form a metal hydride and CO_2 – is important in both organic synthesis[9] and hydrogen storage using organic liquids.[10] There are many examples of metal hydrides that undergo CO_2 insertion,[6] but relatively few in which the kinetics of insertion have been measured.[8a,11]

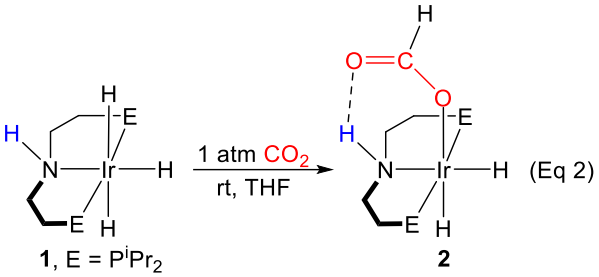

1, E = P^{i}Pr$_2$ **2**

In our early work on CO_2 insertion into metal hydrides we both computationally and experimentally investigated the impact of the ligand *trans* to the hydride on insertion. Initially, we studied CO_2 insertion into pincer supported Ir hydrides of the form (^{Me}PN^{Py}P)IrH$_2$X (^{Me}PN^{Py}P = 2,6-C$_5$NH$_3$(CH$_2$PMe$_2$)$_2$ (**3**); X = anionic donor) to form formate complexes, (^{Me}PN^{Py}P)IrHX{OC(O)H} (**4**), computationally (Figure 1).[1] Our results showed that even when a hydride, one of the strongest *trans*-influence ligands, is opposite to the hydride undergoing CO_2 insertion, the reaction is slightly thermodynamically unfavorable. This demonstrates the challenges associated with promoting CO_2 insertion into third-row transition metal hydrides,[6] which tend to form strong metal hydride bonds. The slightly thermodynamically unfavorable nature of CO_2 insertion into (^{Me}PN^{Py}P)IrH$_3$ also contributes to the outstanding performance of the related complex (^{iPr}PN^{Py}P)IrH$_3$ (^{iPr}PN^{Py}P = 2,6-C$_5$NH$_3$(CH$_2$P^{i}Pr$_2$)$_2$) for CO_2 hydrogenation to

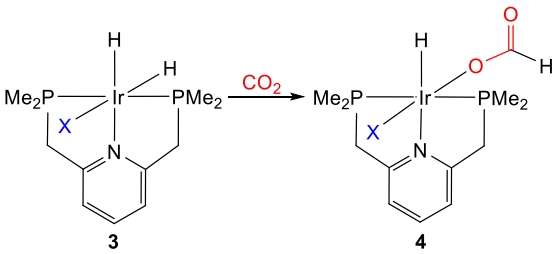

Trans-substituent (X)	ΔG (kcal mol^{-1})
H	0.75
Ph	1.12
Me	1.43
OH	11.1
Cl	19.7
I	20.9

Figure 1: Calculated thermodynamic driving force for CO_2 insertion into a pincer supported Ir hydride as the ligand *trans* to the hydride is varied.

formate because the relatively flat energy profile avoids the formation of low energy intermediates during catalysis.[7] To make CO_2 insertion into an Ir hydride more thermodynamically favorable, we utilized an Ir hydride, **1**, with a modified pincer ligand that was able to hydrogen bond to a bound formate ligand, which created a driving force for insertion (Eq 2).[1] We were able to isolate the formate complex **2**, but **1** gave lower activity for CO_2 hydrogenation to formate than (^{iPr}PN^{Py}P)IrH$_3$ presumably because the favorability of CO_2 insertion created a thermodynamic sink.

We subsequently extended our studies of the impact of the donor *trans* to the hydride on CO_2 insertion to pincer supported Ni and Pd complexes (Figure 2).[12] We showed that CO_2 insertion into PNP supported hydrides, with a relatively weak anionic nitrogen donor *trans* to the hydride, did not occur, while insertion into PCP and PSiP ligated hydrides, with anionic carbon and silicon donors *trans* to the hydride, did occur. Calculations established that the observed reactivity was related to thermodynamic factors and the predicted kinetic barriers were correlated with thermodynamic trends. Overall, this experimental work provided qualitative information about how to control the thermodynamic favorability of CO_2 insertion.

The major reason for our and others inability to gain quantitative information about CO_2 insertion into metal hydrides was that the rates were too rapid to measure using conventional techniques, such as NMR or UV-Vis spectroscopy. To solve this challenge, we used a stopped-flow instrument with a UV-Vis detector to determine the kinetics of CO_2 insertion.[2] This technique enabled the measurement of the rate of reactions that are complete in less than one second at room temperature. We started by studying CO_2 insertion into **1** to form **2** and (^{R}PCP)NiH (^{R}PCP = 2,6-C$_6$H$_3$-

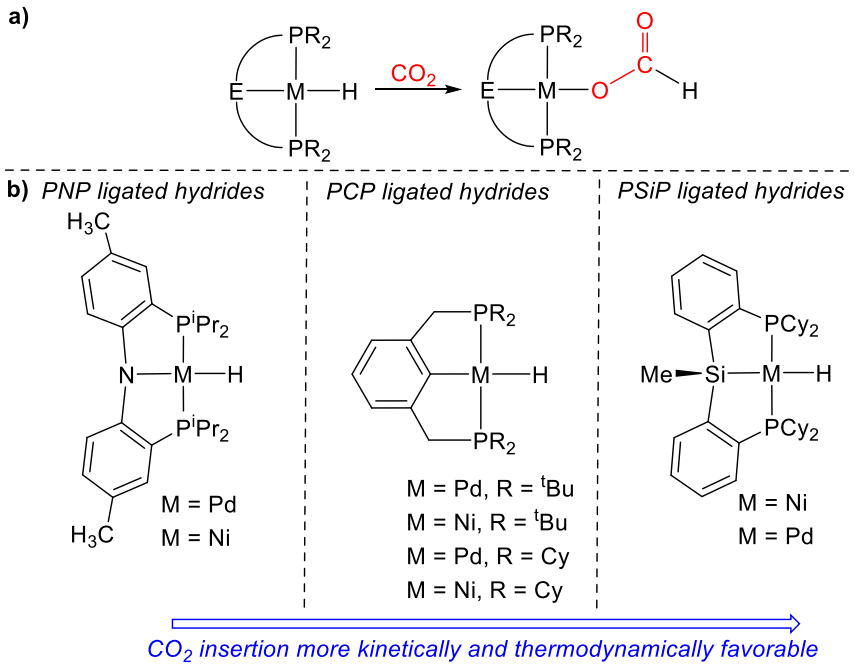

Figure 2: a) Generic scheme for CO_2 insertion into a pincer ligated metal hydride. **b)** Relative reactivity of pincer ligated Ni and Pd hydrides with CO_2.

$(CH_2PR_2)_2$; R = ^{i}Pr, Cy, or ^{t}Bu; **5^{R}**) to form (^{R}PCP)Ni{OC(O)H} (**6^{R}**). We selected these systems because we had previously used them for qualitative studies and DFT investigations suggested that the rate-determining step for insertion was slightly different for **1** and **5** (Figure 3).[1,12a] Specifically, both systems were proposed to react via a two-step pathway involving: (i) nucleophilic attack of the hydride on electrophilic CO_2 to form a zwitterionic H-bound formate, and (ii) rearrangement of the H-bound formate to form the O-bound formate. However, for **1**, step (i) was proposed to be rate-determining, whereas for **3**, step (ii) was proposed to be rate-determining. When step (i) is rate-determining the reaction is described as an outersphere process because there is no interaction between the metal and CO_2 in the rate-determining step, whereas when step (ii) is rate-determining the reaction is referred to as innersphere. Prior to our work innersphere and outersphere processes had predominantly been explored computationally[13] and it was unclear if their rates would be affected differently by changing the ancillary ligand, solvent, or additive in the reaction. It is

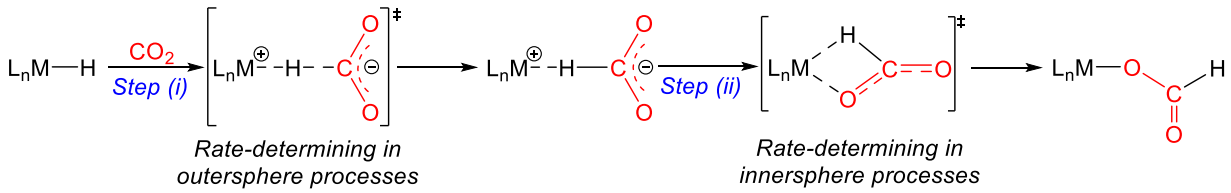

Figure 3: Stepwise pathway for CO_2 insertion into a metal hydride. The rate-determining transition state for an innersphere process is analogous to the transition state for concerted CO_2 insertion via a four-membered transition state.

noteworthy that the rate-determining transition state for the innersphere process is analogous to the transition state that is often invoked for concerted CO_2 insertion into a metal hydride via a four-membered transition state with no intermediates.[6] As such, distinguishing between a concerted process and a stepwise innersphere pathway is likely only possible using computational techniques.

Our stopped-flow studies using **5** enabled the elucidation of steric and electronic effects related to CO_2 insertion (Figure 4).[2] Electron-donating ligands increase the rate of the reaction, as changing from a *para*-iodo to *para*- methoxy group on the ^{tBu}PCP ligand increases the rate by a factor of seven. This electronic effect is small compared to steric factors. The rate increases by a factor of approximately 650 when moving from sterically bulky *tert*-butyl phosphine substituents on the ^{tBu}PCP ligand to *iso*-propyl groups. The solvent also influences the rate of the reaction and there is a 30-fold increase in rate when moving from THF to MeCN. The rate constant for CO_2 insertion correlates poorly with the dielectric constant (ε) and instead correlates strongly with the acceptor number (AN) of the solvent, which is a measure of its Lewis acidity.[14] This observation extended

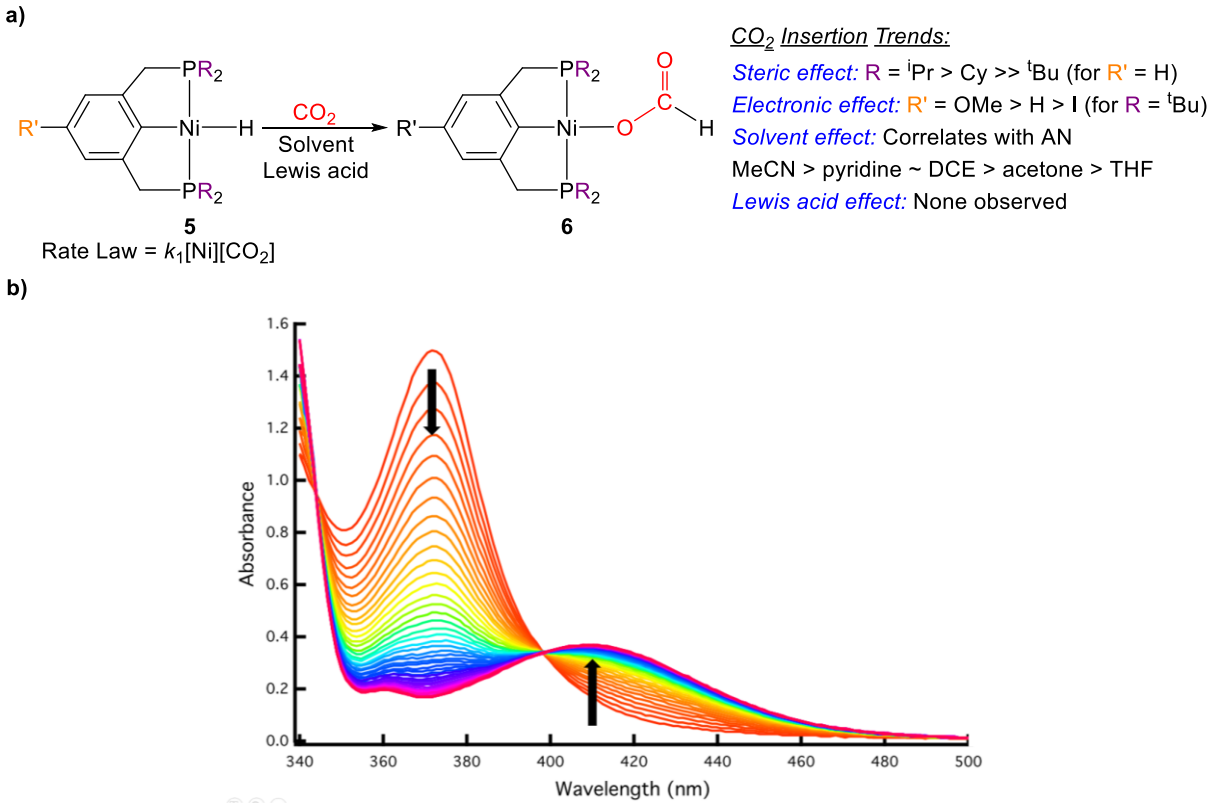

Figure 4: a) Trends in the rate of CO_2 insertion into pincer supported Ni hydrides. **b)** Selected stopped-flow data for the insertion of CO_2 into (^{tBu}PCP)NiH (**5^{tBu}**) to form (^{tBu}PCP)Ni{OC(O)H} (**6^{tBu}**) in benzene at rt. Reaction conditions: [CO_2] = 45 mM, [(^{tBu}PCP)NiH] = 0.3 mM. Total experiment time 6 sec.

reports from previous researchers, which only explored solvents with significantly higher polarity.[11b,11e] The addition of Lewis acids, such as $LiPF_6$, did not result in any change in the rate of CO_2 insertion, which was ascribed to the lack of charge build-up in the rate-determining transition state. However, recent computational studies on a different system suggest that a Lewis acid can stabilize the transition state for conversion from H-bound to O-bound formate and more detailed calculations on this topic are required.[15] Our kinetic studies using **3** provided information on the factors that influence the rate of CO_2 insertion for an innersphere process and the magnitude of the different effects, which provides guidelines on the variables to change in catalysis.

We also measured the kinetics of CO_2 insertion into **1** using a stopped-flow UV-vis spectrophotometer (Figure 5).[2] Due to synthetic challenges, it was not possible to vary the ligand to probe steric and electronic effects. There is a solvent effect on CO_2 insertion into **1**, with the rate increasing by a factor of 29 when moving from diethyl ether to benzene.[2] Although this is

a)

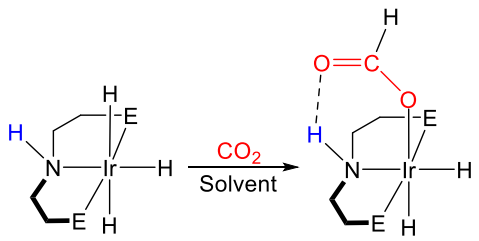

1, E = P^iPr_2 **2**

Rate Law = $k_1[Ir][CO_2]$

CO_2 Insertion Trends:

Solvent effect: No correlation with ε or AN
Benzene > diglyme > 1,4-dioxane > hexane > THF > diethyl ether
Lewis acid effect: Complicated increase in rate observed

b)

Entry	Lewis Acid Additive	k_1 at 273 K[a]	Rate Increase[b]
1	None	64 ± 6	-
2	LiOTf[c]	1.5 (2) x 10^4	9
3	NaOTf	2.4 (2) x 10^4	15
4	$NaNTf_2$[d]	3.0 (3) x 10^4	19
5	$KNTf_2$	4.0 (4) x 10^4	25
6	$LiPF_6$	4.9 (5) x 10^4	30
7	$LiNTf_2$	7.3 (7) x 10^4	46
8	$LiBPh_4$•3 DME[e]	1.2 (1) x 10^5	72
9	$NaBPh_4$	1.3 (1) x 10^5	82
10	$KB(C_6F_5)_4$	1.4 (1) x 10^5	88
11	$NaBAr^F{}_4$[f]	1.6 (2) x 10^5	100

Figure 5: a) Trends in the rate of CO_2 insertion into **1**. **b)** Effect of Lewis acids on the rate of CO_2 insertion into **1** in THF. [a]Entry 1 follows the second order rate law k_1[**1**][CO_2], where k_1 is in M^{-1} s^{-1}; Entries 2-11 follow the third order rate law k_1[**1**][CO_2][LA], where k_1 is in M^{-2} s^{-1}. [b]The rate increase is based on the calculated rate of product formation (M s^{-1}) in the presence of 20 equivalents of LA (relative to [**1**]). [c]OTf = trifluoromethanesulfonate. [d]NTf_2 = bis(trifluoromethane)sulfonamide. [e]$LiBPh_4$•3DME = lithium tetraphenylborate tris(1,2-dimethoxyethane). [f]$NaBAr^F{}_4$ = sodium tetrakis[3,5-bis(trifluoromethyl)phenyl]borate.

similar in magnitude to **5**, the range of solvents studied for **5** was much larger, whereas **1** is unstable in polar solvents. This suggests that solvent effects may be more significant for systems which insert CO_2 via an outersphere mechanism. The rate of CO_2 insertion into **1** does not correlate with the solvent AN, suggesting that this trend is not general. In contrast to **5**, the addition of Lewis acids, such as $LiPF_6$, result in significant enhancements in the rates of CO_2 insertion into **1** and the rate law shows a first-order dependence on Lewis acid. This result is rationalized on the basis that a Lewis acid provides stabilization of the zwitterionic rate-determining transition state in an outersphere process. However, the dependence of the rate on the identity of the Lewis acid is complicated and there is significant variation within a series of anions with the same cation (for example: NaOTf, $NaNTf_2$, $NaBPh_4$, and $NaBAr^F{}_4$; Entries 3, 4, 9, & 11). This effect is proposed to be related to differences in ion-pairing, which lead to a higher concentration of Na^+ from $NaBAr^F{}_4$ than NaOTf in THF. Differences in ion-pairing also prevent comparison of the ability of different cations to stabilize the rate-determining transition state. Nevertheless, this study represented the first quantitative demonstration that Lewis acids could increase the rate of CO_2 insertion into metal hydrides.

To solve problems associated with ion pairing, we measured the rate of CO_2 insertion into the cationic Ru hydride $[Ru(tpy)(bpy)H]PF_6$ (tpy = 2,2':6',2''-terpyridine, bpy = 2,2'-bipyridine, **7**) to form $[Ru(tpy)(bpy)\{OC(O)H\}]PF_6$ (**8**) in various solvents, both in the presence and absence of a Lewis acids (Figure 6).[3] Calculations had previously suggested that pathway for CO_2 insertion into **7** was outersphere.[16] The advantage of **7** compared to **1** is that it undergoes insertion in polar solvents, which allowed us to directly compare the effect of different Lewis acids in the absence of ion pairing effects. Lewis acids enhance the rate of CO_2 insertion into **7** in the order $Li^+ >> Na^+ > K^+ > Rb^+$ and the identity of the anion does not change the rate (Figure 6b). Presumably, the smaller Li^+ cation stabilizes the incipient negative charge on the formate more strongly. Interestingly, more polar solvents generally give smaller Lewis acid effects, so in MeCN the Lewis acid effect is approximately 30 times more pronounced than in methanol. We hypothesize that this is because more polar solvents can also stabilize the zwitterionic transition state and consequently more polar solvents out compete the Lewis acid. Finally, we used the rate constants for CO_2 insertion into **7** to refine our model for predicting solvent effects. We observed that the rate of insertion was approximately 900 times faster in methanol compared with acetone, which again suggests that solvent effects are larger for outersphere systems. Further, the best solvent parameter

for predicting the rate of CO_2 insertion is the Dimroth-Reichardt $E_T(30)$ solvent parameter (Figure 6c).[17] The $E_T(30)$ value is the molar electronic transition energy of the lowest energy

a)

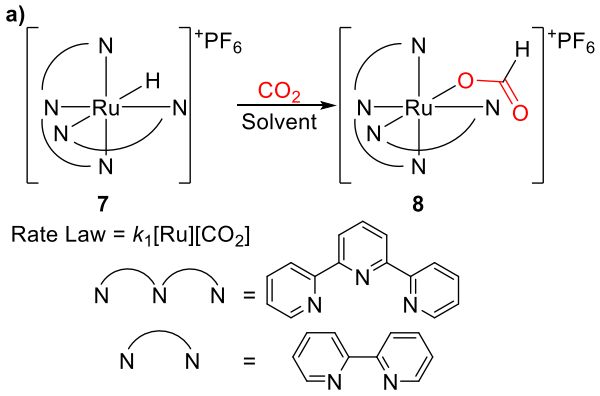

CO_2 Insertion Trends:

Solvent effect: Correlates with $E_T(30)$ parameter
Methanol > ethanol > isopropanol > MeCN > acetone

Lewis acid effect: $Li^+ >> Na^+ > K^+ > Rb^+$ (in MeCN)

b)

Entry	Lewis Acid Additive	Rate Constant (M^{-2} s^{-1}) at rt
1	None	1.0 (1) x 10^{-2} [a]
2	$LiNTf_2$	3.1 ± 0.3
3	LiOTf	3.0 ± 0.3
4	$LiBPh_4$·3DME	3.0 ± 0.3
5	$NaBAr^F_4$	4.0 (4) x 10^{-1}
6	NaOTf	4.0 (4) x 10^{-1}
7	$NaBPh_4$	3.7 (4) x 10^{-1}
8	$NaNTf_2$	3.4 (3) x 10^{-1}
9	KPF_6	2.5 (3) x 10^{-1}
10	$KBPh_4$	2.1 (2) x 10^{-1}
11	$KNTf_2$	2.0 (2) x 10^{-1}
12	$KB(C_6F_5)_4$	1.9 (2) x 10^{-1}
13	$RbBPh_4$	1.0 (1) x 10^{-2}

c)

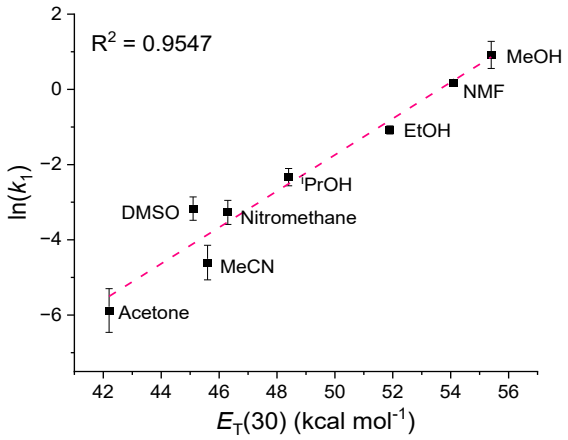

Figure 6: a) Trends in the rate of CO_2 insertion into **7**. **b)** Effect of Lewis acids on the rate of CO_2 insertion into **7** in MeOH. [a]Entry 1 lists the bimolecular rate constant for CO_2 insertion in units of M^{-1} s^{-1}. **c)** Relationship between the second-order rate constant k_1 for CO_2 insertion into **7** in various solvents and the Dimroth-Reichardt $E_T(30)$ value of the solvent.

intramolecular charge-transfer π-π* absorption band of a negatively solvatochromic pyridinium *N*-phenolate betaine dye in that particular solvent and has been measured for over 350 solvents as well as numerous binary solvent mixtures. Importantly, the $E_T(30)$ value gives a better correlation with the rate constant for CO_2 insertion than the AN (or the dielectric constant) of the solvent, which was the previous best predictor of the rate of CO_2 insertion for a given solvent, and is our preferred solvent property for predicting rates.

We were unable to study ligand effects in outersphere CO_2 insertion using **1** and **7**. Therefore, we measured the kinetics of CO_2 insertion into (^{R}bpy)$Re(CO)_3H$ (bpy = 4,4'-R-2,2'-bipyridine; R =

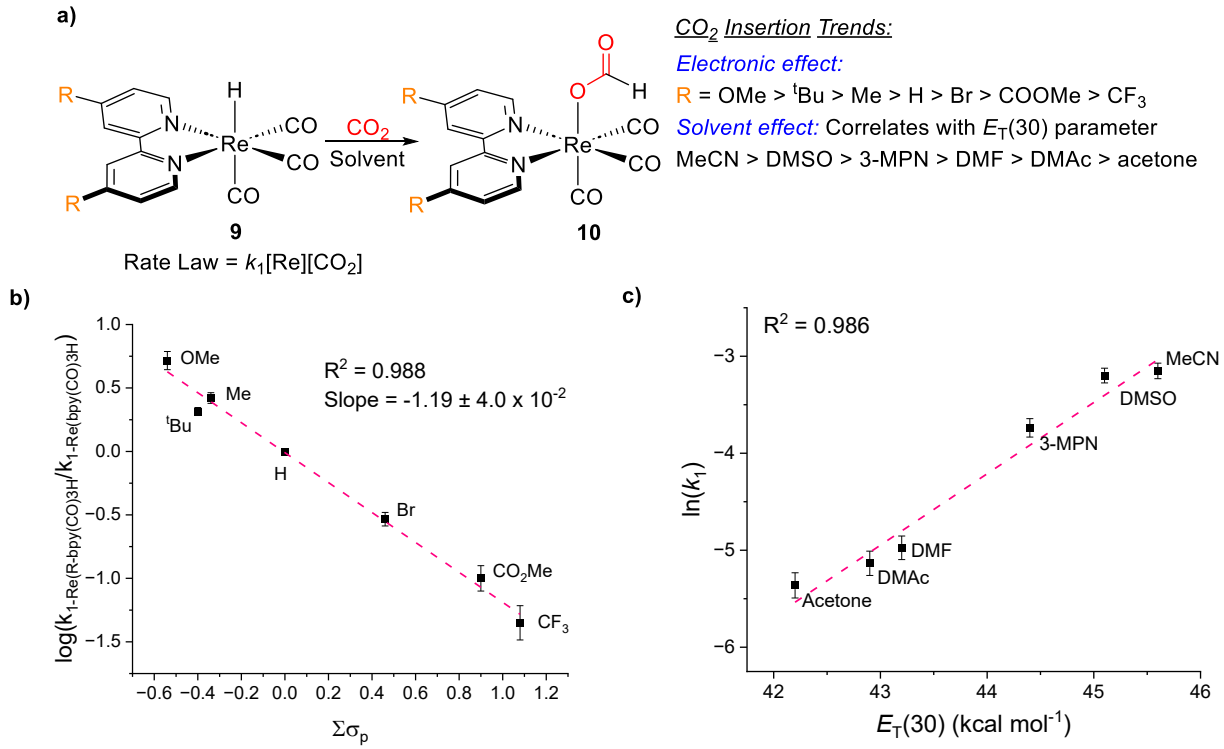

Figure 7: a) Trends in the rate of CO_2 insertion into **9**. **b)** Hammett plot for CO_2 insertion into (^{R}bpy)Re(CO)$_3$H. **c)** Relationship between the second-order rate constant k_1 for CO_2 insertion into (^{R}bpy)Re(CO)$_3$H in various solvents and the Dimroth-Reichardt $E_T(30)$ value of the solvent.

OMe, ^{t}Bu, Me, H, Br, COOMe, CF_3, **9**) to form the formate complexes (^{R}bpy)Re(CO)$_3${OC(O)H)} (**10**) (Figure 7a).[18] The kinetics of CO_2 insertion into similar compounds had previously been explored by Sullivan and Meyer[11a] and DFT calculations predicted an outersphere pathway.[18] When comparing the rate constants for CO_2 insertion between the most electron-donating hydride, (^{OMe}bpy)Re(CO)$_3$H, and the least electron-donating hydride, (^{CF3}bpy)Re(CO)$_3$H, there is a difference of more than two orders of magnitude. The electron-rich ligand promotes insertion presumably by stabilizing the positive charge build-up on the metal center, which is expected in an outersphere process. We also generated a Hammett plot for CO_2 insertion into our electronically diverse Re hydrides, which gave a negative slope of -1.19 (Figure 7b). To understand the impact of solvent on the rates of CO_2 insertion into **9**, we measured the kinetics of insertion in MeCN, acetone, dimethylacetamide (DMAc), dimethylformamide (DMF), dimethylsulfoxide (DMSO), and 3-methoxypropionitrile (3-MPN).[19] We observe an excellent correlation between the rate constant for CO_2 insertion into any single Re complex (for example (bpy)Re(CO)$_3$H or (^{OMe}bpy)Re(CO)$_3$H) and the $E_T(30)$ parameter of the solvent (Figure 7c). This provides further support that the solvent $E_T(30)$ parameter is the best predictor of the rate of insertion in a given

solvent. For our series of complexes (^{R}bpy)Re(CO)$_3$H in different solvents a negative Hammett plot was observed in all cases, but there were no trends in the slope of the Hammett plot as the solvent was varied.

Our quantitative studies on CO_2 insertion into metal hydrides allow us to make several general conclusions: (i) The rate laws for CO_2 insertion reactions are normally first-order in the concentrations of both metal complex and CO_2. (ii) The rate constants for CO_2 insertion typically range from 10^{-4} to 10^{2} M^{-1} s^{-1}, which means that a stopped-flow instrument is normally required to measure kinetics. (iii) In all cases negative values of $\Delta S^{\ddagger}$ (typically ranging from -20 to -50 cal mol^{-1} K^{-1}) are observed, consistent with a rate-determining transition state which involves two molecules combining to form an adduct. There are no discernable trends in the entropies of activation based on the reaction pathway. (iv) Inverse kinetic isotope effects (KIEs) are observed in all systems, when the metal hydride is changed to a metal deuteride. This is in agreement with the C–H bond that is formed being stronger than the M–H bond that is broken. The magnitude of the KIEs ranges from 0.6-0.8, with no correlation between the proposed reaction pathway and the KIE values. (v) More electron-donating ancillary ligands promote CO_2 insertion into both innersphere and outersphere systems, but more work is required to determine if there are differences in magnitude between the pathways. (vi) The Dimroth-Reichardt parameter of a solvent correlates strongly with the rate constant for CO_2 insertion. Solvent effects are larger for an outersphere process compared to an innersphere process. (vii) The rates of CO_2 insertion for complexes that react via an outersphere pathway can be increased by the addition of a Lewis acid, but the magnitude of the Lewis acid effect is influenced by the polarity of the solvent. Larger Lewis acid effects are observed in less polar solvents. Lewis acids do not change the rates of insertion for systems that react via an innersphere pathway.

Taken together, our results provide guidelines for modulating the rates of CO_2 insertion and experimentally distinguishing between inner and outersphere pathways based on observed trends. However, our kinetics do not establish that intermediates are present in CO_2 insertion reactions and cannot be used to distinguish between concerted or stepwise processes. Although calculations suggest a stepwise process, it is feasible that differences between early and late transition states in a concerted process cause the observed effects in our kinetic studies. Further, in some cases calculations from independent groups have reached different conclusions about whether reactions

are inner or outersphere.[18,20] To address this issue, more extensive modelling is required to show that a proposed pathway can reproduce all observed solvent and Lewis acid effects, as well as KIEs. The conclusions from these higher-level calculations may change the interpretation of experimental results.

The low barriers for CO_2 insertion into a metal hydride that we observe indicate that in catalytic reactions involving the complexes we have studied, insertion is unlikely to be turnover limiting. However, there are transition metal mediated CO_2 hydrogenation reactions where CO_2 insertion is proposed to be turnover limiting, such as catalysis with $(dmpe)_2CoH$ (dmpe = 1,2-bis(dimethylphosphino)ethane) and our results about controlling the rates of insertion are likely transferable to these systems.[21] Further, even in cases where CO_2 insertion is not turnover limiting, it can still be important to increase the rate of CO_2 insertion into a metal hydride to improve selectivity. For example, CO_2 insertion may compete with unwanted generation of H_2 from protonation of the metal hydride.[8b] Finally, in catalytic reactions that involve the microscopic reverse elementary step to CO_2 insertion into a metal hydride, decarboxylation of a metal formate to generate a metal hydride, this step can be rate-determining,[10] and our results will provide information on how to increase the rates of this transformation.

Carbon Dioxide Insertion into Nickel and Palladium Alkyl Bonds

The National Academies of Science recently identified the formation of products containing a C–C bond from CO_2 as a high priority research area.[22] Understanding the insertion of CO_2 into a metal-alkyl bond is likely important to achieving this goal, as it is an elementary step that results in the formation of C–C bonds. Several Group 10 catalysts for the reductive carboxylation of alkyl halides and pseudo halides have already been developed, in which CO_2 insertion into a metal alkyl

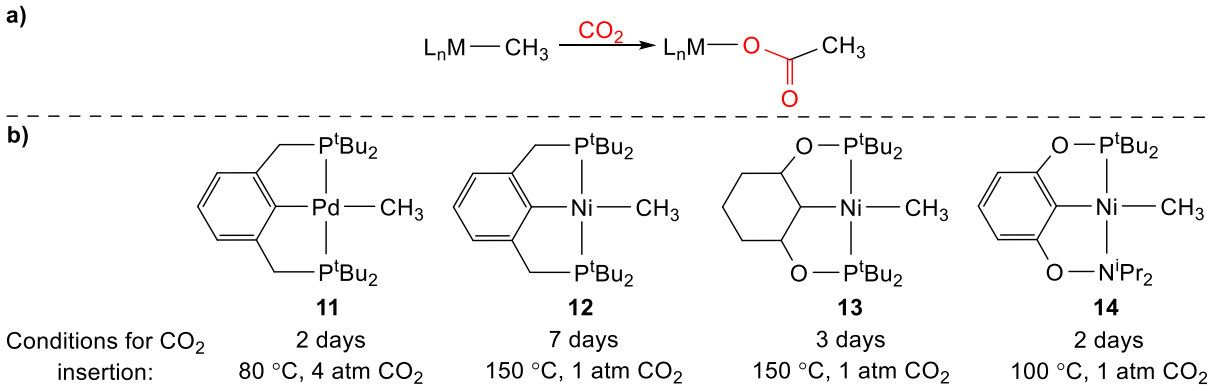

Figure 8: a) Generic scheme for CO_2 insertion into a metal methyl complex. **b)** Pincer ligated methyl complexes that undergo CO_2 insertion.

bond is proposed to be a key step.[23] However, although there are many examples of CO_2 insertion into metal alkyl bonds using both early and late transition metals, kinetic studies that help to understand the impact of the metal, ancillary ligand, or solvent, are rare.[11d,24] Consequently, it was unclear how to promote CO_2 insertion, which hinders catalyst development.

Historically, CO_2 insertion reactions into Group 10 metal alkyls have required elevated temperatures, which led to a focus on pincer supported complexes that often have high thermal stability. For instance, Wendt and co-workers showed that the reaction of (^{tBu}PCP)Pd(CH_3) (**11**) with 4 atm of CO_2 at 80 °C results in the formation of the κ^1-acetate complex (^{tBu}PCP)Pd{OC(O)CH_3}, but the reaction takes two days (Figure 8).[25] We demonstrated that the reaction of 1 atm of CO_2 with the related compound (^{tBu}PCP)Ni(CH_3) (**12**) requires heating to 150 °C to form (^{tBu}PCP)Ni{OC(O)CH_3}, but several by-products were also observed.[12a] Subsequently, Wendt reported that changing the pincer ligand from ^{tBu}PCP to a pincer ligand with an sp^3-hybridized carbon central donor, **13**, or replacing one of the phosphine arms of the pincer ligand with a nitrogen donor, **14**, does not lead to significant changes in the rate of CO_2 insertion.[26] The only Group 10 alkyl complexes that undergo CO_2 insertion under mild conditions are an unstable anionic Pd complex[27] and several Ni^I complexes,[28] which are also relatively unstable. This has prevented detailed kinetic studies.

Based on the trends we elucidated for CO_2 insertion into metal hydrides,[12b] we hypothesized that Group 10 alkyl complexes with a more strongly donating ligand *trans* to the metal alkyl would insert CO_2 under milder conditions. Therefore, we synthesized Group 10 methyl complexes of the type (^{R}PBP)M(CH_3) (^{R}PBP = C_6H_4-1,2-(NCH_2PR_2)B^-; R = Cy or ^{t}Bu; M = Ni or Pd; **15**), which contain a central boryl donor that exerts a strong *trans*-influence opposite the hydride.[4,29] Treatment of (^{Cy}PBP)Pd(CH_3) or (^{tBu}PBP)Pd(CH_3) with 1 atm of CO_2 results in the quantitative formation of the κ^1-acetate complexes (^{Cy}PBP)Pd{OC(O)CH_3} or (^{tBu}PBP)Pd{OC(O)CH_3} (**16**) in one hour and six hours at room temperature, respectively (Figure 9).[4] In contrast, CO_2 insertion

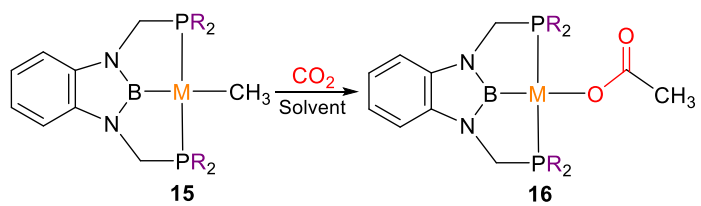

CO_2 Insertion Trends:
Metal effect: M = Pd > Ni
Steric effect: R = Cy > ^{t}Bu
Solvent effect: Correlates with $E_T(30)$ parameter
Glyme > THF > 1,4-dioxane > benzene > toluene
Lewis acid effect: None observed

Figure 9: Trends in the rate of CO_2 insertion into (^{R}PBP)M(CH_3).

reactions into (^{R}PBP)Ni(CH_3) were not clean and significantly slower. For example, the reaction with the ^{Cy}PBP-ligated species reached completion after four days at room temperature. From these initial experiments and associated DFT calculations (Table 1), we concluded that: (i) increasing the *trans*-influence of the donor opposite the methyl group results in faster CO_2 insertion. (ii) Pd methyl complexes undergo faster insertion than Ni methyl complexes, which is the opposite trend compared to Ni and Pd hydrides. (iii) Increasing the steric bulk around the complexes leads to slower insertion.

Detailed kinetic analysis of CO_2 insertion into (^{tBu}PBP)Pd(CH_3) revealed that the reaction is first-order in [Pd] and [CO_2].[4] The negative entropy of activation, -32.2 ± 3.2 cal mol^{-1} K^{-1} is consistent with a rate-limiting transition state in which two molecules are combining to form an adduct. Although (^{tBu}PBP)Pd(CH_3) is only stable in a limited number of ethereal and hydrocarbon based solvents, we demonstrated that the rate of CO_2 insertion correlates well with the $E_T(30)$ parameter of the solvent. The variation in rate constant on changing solvent is significantly smaller than that observed for the Ir hydride, **1**, suggesting that there is less charge build-up in the transition state for insertion into (^{tBu}PBP)Pd(CH_3). Consistent with this observation no increase in rates was observed due to the presence of Lewis acids, such as $LiPF_6$, although increasing the ionic strength of the solution results in a small enhancement.

Almost all studies measuring the kinetics of CO_2 insertion into alkyl complexes have focused on metal methyl species[30] because longer chain alkyl complexes are often unstable due to their propensity to undergo β-hydride elimination. Given that pincer ligands inhibit β-hydride elimination from square planar Pd^{II} complexes,[31] we were able to isolate (^{tBu}PBP)Pd(CH_2CH_3) and (^{tBu}PBP)Pd($CH_2CH_2CH_3$), as well as the related benzyl complexes (^{tBu}PBP)Pd($CH_2C_6H_5$) and (^{tBu}PBP)Pd(CH_2-4-OMe-C_6H_4).[32] Kinetic studies revealed that the rate for CO_2 insertion into the ethyl complex to form an acetate complex is remarkably *more than double* the rate of CO_2 insertion into the methyl species, while insertion into the n-propyl complex to form the corresponding carboxylate occurs at approximately one-tenth the rate of the methyl species (Figure 10). The

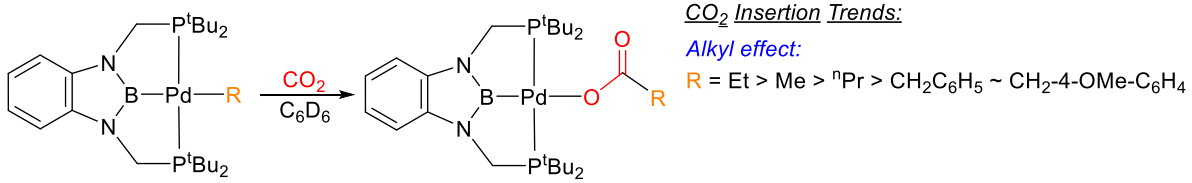

Figure 10: Trends in the rate of CO_2 insertion into (^{tBu}PBP)Pd(alkyl).

insertion of CO_2 into the benzyl complexes is significantly slower than any of the n-alkyl complexes, but the substituent on the benzyl group does not impact the rate.

To understand the observed experimental trends and the pathway for CO_2 insertion into complexes of the type (^{tBu}PBP)Pd(alkyl), we performed DFT calculations.[4,32] For insertion into (^{tBu}PBP)Pd(CH_3), our calculations indicate that a two-step S_E2 mechanism is the lowest energy pathway (Figure 11a, Table 1). The first step is rate-determining and involves the nucleophilic attack of the methyl group on CO_2 without any direct interaction between Pd and CO_2. The second step involves rearrangement of an acetate that is bound through a C–H sigma bond to generate the O-bound product. This pathway is essentially analogous to the outersphere pathway for CO_2 insertion into a metal hydride, but the barriers are higher ($\Delta G^{\ddagger}$ is ~20 kcal mol^{-1} for methyl compared to 12-16 kcal mol^{-1} for hydride) because of the lower nucleophilicity of the methyl compared to a hydride. A concerted mechanism involving direct 1,2-insertion was also calculated and is approximately 6 kcal mol^{-1} higher in energy for (^{tBu}PBP)Pd(CH_3) (Figure 11b, Table 1). When a calculation was performed with the model complex (^{Me}PBP)Pd(CH_3) the concerted pathway is lower in energy than the stepwise pathway, suggesting that the steric bulk around the Pd center influences the reaction mechanism.

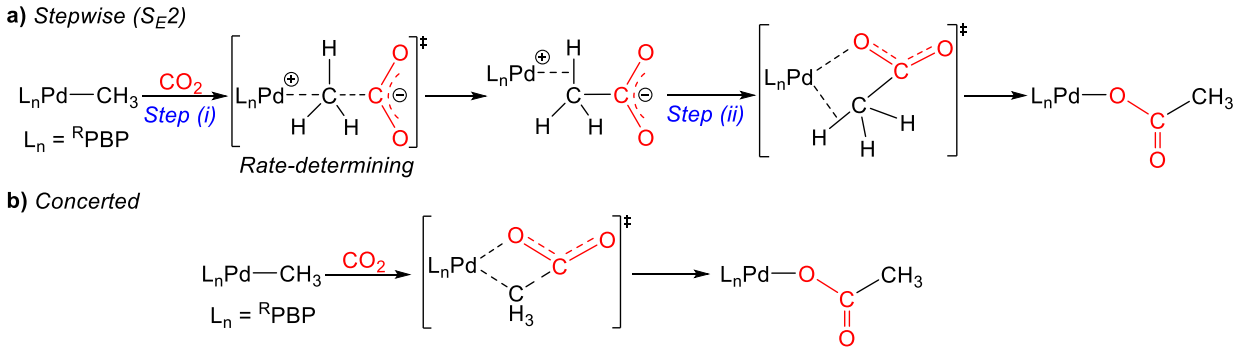

Figure 11: Representations of the stepwise (S_E2) (**a**) and concerted (**b**) pathways for CO_2 insertion into (^{R}PBP)Pd(CH_3).

Complex	$\Delta G^{\ddagger}$ Stepwise (kcal mol^{-1})	$\Delta G^{\ddagger}$ Concerted (kcal mol^{-1})
(^{tBu}PBP)Pd(CH_3)	**19.0**	25.1
(^{Me}PBP)Pd(CH_3)	22.5	**19.4**
(^{tBu}PBP)Ni(CH_3)	**24.5**	31.9
(^{tBu}PCP)Pd(CH_3)	**24.2**	36.7
(^{Me}PCP)Pd(CH_3)	26.8	**25.0**

Table 1. Calculated free energy barriers for stepwise and concerted CO_2 insertion into pincer-supported Pd and Ni methyl complexes.

Insertion into (^{tBu}PBP)Pd(CH_2CH_3), (^{tBu}PBP)Pd($CH_2CH_2CH_3$), (^{tBu}PBP)Pd($CH_2C_6H_5$), and (^{tBu}PBP)Pd(CH_2-4-OMe-C_6H_4) were also calculated to proceed via an S_E2 pathway.[32] Calculations were able to reproduce the lower barrier for (^{tBu}PBP)Pd(CH_2CH_3) relative to (^{tBu}PBP)Pd(CH_3), as well as the higher barrier for (^{tBu}PBP)Pd($CH_2CH_2CH_3$). Steric factors are proposed to be responsible for the differences in rates and calculations using a model system with less steric bulk, (^{iPr}PBP)Pd(alkyl), indicate that the barriers change in the order methyl < ethyl < propyl. This is expected to be the trend for most alkyl systems, but the steric congestion imposed by the ^{tBu}PBP ligand make it an outlier. The S_E2 pathway is also consistent with the slower rate of insertion observed for Pd benzyl complexes compared with Pd n-alkyl complexes. The benzylic carbon bound to Pd is a worse nucleophile because of the electron-withdrawing nature of the aromatic group. This causes the initial attack on electrophilic CO_2 to be less favorable. However, it is surprising that no differences in rates are observed for (^{tBu}PBP)Pd($CH_2C_6H_5$) and (^{tBu}PBP)Pd(CH_2-4-OMe-C_6H_4).

Our studies have implications for catalytic reactions where CO_2 insertion into a Group 10 alkyl bond is a key step in catalysis, such as the carboxylation of alkyl halides.[23] They suggest: (i) that the nature of the alkyl group (methyl *vs* benzyl) is likely to significantly impact the rate of insertion and the ancillary ligand or reaction conditions may need to be changed depending on the alkyl substrate. (ii) Changing the nature of the solvent to one with a higher $E_T(30)$ value can be used to increase the rate of CO_2 insertion. (iii) At least for Ni^{II} and Pd^{II} systems, CO_2 insertion into the metal alkyl bond is a challenging reaction and further work to understand how to improve the rates is required. This could involve the use of additives, which are often present in catalysis.[23] It is also noteworthy that our studies of the kinetics of CO_2 insertion into Ni and Pd methyl groups have focused on Ni^{II} and Pd^{II} systems, and in some catalytic reactions CO_2 insertion into Ni^{I} alkyl complexes is proposed.[23] The kinetics of these reactions has not been probed, in part due to the instability of Ni^{I} complexes,[28b] and understanding the similarities and differences between insertion into Ni^{I} and Ni^{II} alkyl complexes would be valuable.

Carbon Dioxide Insertion into Metal Amides and Alkoxides

There is interest in understanding the pathway for CO_2 insertion into metal hydroxides and amides.[33] Carbonic anhydrase enzymes convert CO_2 and H_2O into bicarbonate (and H^+) via a mechanism that is proposed to involve CO_2 insertion into a Zn–OH bond,[34] while CO_2 insertion

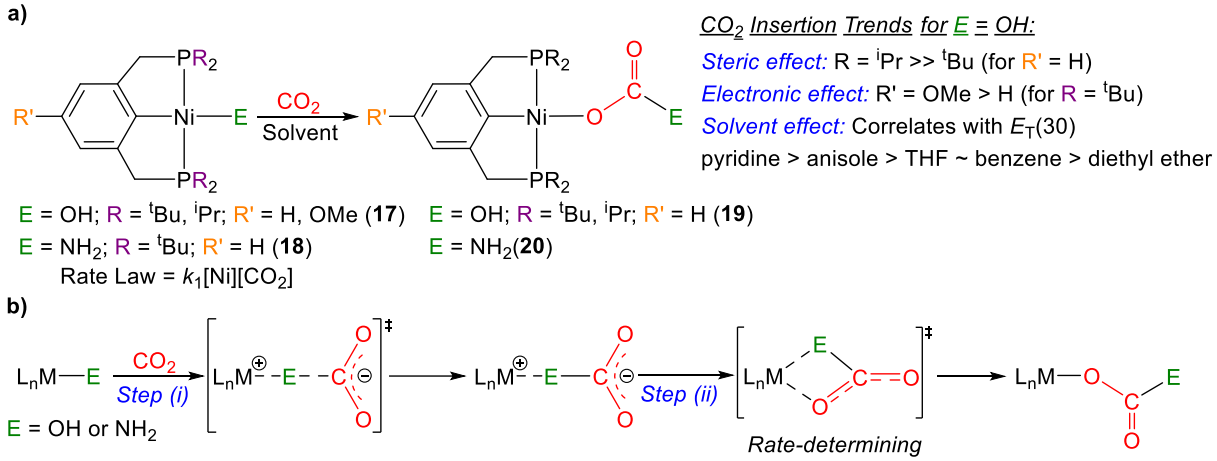

Figure 12: a) Trends in the rate of CO_2 insertion into pincer supported Ni hydroxides and amides. **b**) Proposed mechanism for CO_2 insertion into metal hydroxides and amides.

into transition metal amides is a key step in the preparation of ureas and carbamates from CO_2 and amines.[35] We initially demonstrated CO_2 insertion into (^{tBu}PCP)Ni(OH) (**17**) and (^{tBu}PCP)Ni(NH_2) (**18**) to form (^{tBu}PCP)Ni{OC(O)OH} (**19**) and (^{tBu}PCP)Ni{OC(O)NH_2} (**20**), respectively (Figure 12a).[36] The kinetics of the reactions were too fast to measure using conventional methods but a stopped-flow instrument enabled the rates of CO_2 insertion into (^{R}PCP)Ni(OH) to be determined,[37] in a similar fashion to previous studies from Holm and co-workers.[33] However, even with a stopped-flow instrument, insertion into **18** was too fast to measure. The insertion of CO_2 into (^{tBu}PCP)Ni(OH) is between 600 and 14,000 times faster than insertion into (^{tBu}PCP)NiH depending on the solvent, but the trends were similar. For example, the rate of insertion into (^{R}PCP)Ni(OH) increased with more electron-donating substituents on the pincer ligand, while less sterically bulky substituents on the phosphine donors also increased the rate. Further as the solvent was changed, the rates of insertion correlated with the $E_T(30)$ value of the solvent. In all cases the effect was smaller for (^{tBu}PCP)Ni(OH) than (^{tBu}PCP)NiH (**5^{tBu}**).

The calculated pathways for CO_2 insertion into (^{tBu}PCP)Ni(OH) and (^{tBu}PCP)Ni(NH_2) are analogous to those determined for (^{tBu}PCP)NiH (Figure 12b).[36] The first step involves nucleophilic attack of the hydroxide or amide on CO_2. These processes have a low barrier due to the nucleophilicity of the hydroxide or amide ligand. In the second and rate-determining step the carbonate or carbamate ligand rearranges to be bound through an X-type oxygen ligand. Consistent with our experimental results the barrier for carbamate rearrangement is lower than carbonate rearrangement ($\Delta G^{\ddagger}$ = 7.9 *vs* 12.2 kcal mol^{-1}), which is presumably partially related to the

thermodynamic driving force for formation of the carbamate product being ~9 kcal mol^{-1} greater than formation of the carbonate product. In the rate-determining transition state for CO_2 insertion into (^{tBu}PCP)Ni(OH) there is less charge build-up on the Ni center compared to (^{tBu}PCP)NiH, which is in agreement with the smaller solvent and ancillary ligand effects. Given the substantially lower barrier for CO_2 insertion into (^{tBu}PCP)Ni(OH) compared to (^{tBu}PCP)NiH, which we propose is general to other systems, CO_2 insertion into a hydroxide will be kinetically preferred in a catalytic reaction containing both a metal hydroxide and a metal hydride. This is particularly relevant to CO_2 hydrogenation reactions in aqueous environments.[7] However, CO_2 insertion into both metal hydroxide and hydrides is typically reversible so thermodynamic factors are likely to govern selectivity in catalysis. Overall, given the facile nature of CO_2 insertion into metal amides and hydroxides, these steps are unlikely to represent the turnover limiting step in catalysis. Nevertheless, modulating their rates may be crucial to improving selectivity.

Conclusions

Our studies show that there are experimental trends for CO_2 insertion into metal-element σ-bonds that are general for hydrides, alkyls, hydroxide, and amides. These include: (i) electron-donating ancillary ligands increase the rate of insertion by stabilizing the positive charge that is present on the metal center in the rate-determining transition state. (ii) The presence of a donor ligand with a higher *trans*-influence opposite the metal-element σ-bond results in faster insertion. (iii) Insertion reactions are entropically disfavored. (iv) The rate constants for insertion in different solvents correlate with the $E_T(30)$ value of the solvent. However, the magnitude of these effects varies depending on the metal-element σ-bond and the exact pathway for CO_2 insertion.

The most common pathway for insertion involves initial nucleophilic attack of the element in the metal-element σ-bond on CO_2 followed by rearrangement to generate an oxygen bound product. For metal-element σ-bonds involving an element that is not very nucleophilic, for example alkyl ligands, the first step is rate-determining. For systems containing an element that is nucleophilic, for example amide or hydroxide ligands, which contain a lone pair, the second step is rate-determining. In the case of hydrides, which step is rate-determining depends on the metal and the ancillary ligand. Generally, the rates of insertion follow the trend *amide* > *hydroxide* > *hydride* > *alkyl*, which suggests there is a positive correlation between the nucleophilicity of the element in the metal-element σ-bond and the rate of insertion. Reactions in which there is more significant

charge build-up on the metal in the rate-determining transition state tend to have larger solvent effects. For metal hydrides, we hypothesize that the rates of insertion reactions that proceed through an outersphere pathway can be increased through the addition of Lewis acids, while reactions that proceed through an innersphere pathway show no impact from Lewis acids. To date no computational work has been able to reproduce all of our experimental trends relating to ancillary ligand, Lewis acid, and solvent effects, as well as KIEs, and further work is required to fully comprehend the impact on these factors on reaction intermediates. Nevertheless, our current level of understanding provides a plethora of information about how to control the favorability and rates of CO_2 insertion reactions.

It is noteworthy that the results described in this *Account* not only provide guidance about how to optimize CO_2 insertion reactions but are also relevant to related transformations. For example, we have demonstrated that the trends observed for outersphere CO_2 insertion into a metal hydride are also relevant to catalytic ionic hydrogenation,[18] where hydride transfer from a metal hydride to an organic acceptor is a crucial step.[38] Specifically, in both cases there are related linear free energy relationships between kinetic hydricity, the rate constant for the reaction, and thermodynamic hydricity, the driving force for the metal hydride to give up H^-.[18] Given that CO_2 shares some chemical properties with organic carbonyls, it is likely that methods to control CO_2 insertion will also be relevant to some reactions between transition metal hydrides and substrates such as aldehydes, ketones, and amides.

Author Biographical Details

Nilay Hazari gained B.Sc. (1999-2002) and M.Sc. (2003) degrees at the University of Sydney under the supervision of Dr. Les Field. He subsequently completed a D. Phil (2006) at the University of Oxford as a Rhodes Scholar under the supervision of Dr. Jenny Green. He concluded his training as a Postdoctoral Scholar at the California Institute of Technology working with Dr. John Bercaw and Jay Labinger. Dr. Hazari is currently the John Randolph Huffman Professor of Chemistry and Department Chair in the Chemistry Department at Yale University. His research group focuses on using mechanistic studies to develop transition metal catalysts.

Acknowledgements

I acknowledge support from National Science Foundation through Grants CHE-1953708 and CHE-2347883 and the Yale Center for Natural Carbon Capture. I am grateful to Dr. Xiaofan Jia

and Dr. Abhishek Kumar for assistance with generating figures, Dr. Jose Alvarez-Hernandez and Devi Oniani for comments, and all co-workers and collaborators, who have contributed to the work described in this *Account*.

Competing Financial Interests

The author declares no competing financial interests.

References

1. Schmeier, T. J.; Dobereiner, G. E.; Crabtree, R. H.; Hazari, N. Secondary Coordination Sphere Interactions Facilitate the Insertion Step in an Iridium(III) CO_2 Reduction Catalyst. *J. Am. Chem. Soc.* **2011**, *133*, 9274.
2. Heimann, J. E.; Bernskoetter, W. H.; Hazari, N.; Mayer, J. M. Mechanism-Dependent Lewis Acid and Solvent Effects on CO_2 Insertion into Metal Hydrides. *Chem. Sci.* **2018**, *9*, 6629.
3. Heimann, J. E.; Bernskoetter, W. H.; Hazari, N. Understanding the Individual and Combined Effects of Solvent and Lewis Acid on CO_2 Insertion into a Metal Hydride. *J. Am. Chem. Soc.* **2019**, *141*, 10520.
4. Deziel, A. P.; Espinosa, M. R.; Pavlovic, L.; Charboneau, D. J.; Hazari, N.; Hopmann, K. H.; Mercado, B. Q. Ligand and Solvent Effects on CO_2 Insertion into Group 10 Metal Alkyl Bonds. *Chem. Sci.* **2022**, *13*, 2391.
5. (a) Appel, A. M.; Bercaw, J. E.; Bocarsly, A. B.; Dobbek, H.; DuBois, D. L.; Dupuis, M.; Ferry, J. G.; Fujita, E.; Hille, R.; Kenis, P. J. A.; Kerfeld, C. A.; Morris, R. H.; Peden, C. H. F.; Portis, A. R.; Ragsdale, S. W.; Rauchfuss, T. B.; Reek, J. N. H.; Seefeldt, L. C.; Thauer, R. K.; Waldrop, G. L. Frontiers, Opportunities, and Challenges in Biochemical and Chemical Catalysis of CO_2 Fixation. *Chem. Rev.* **2013**, *113*, 6621; (b) Wang, W.-H.; Himeda, Y.; Muckerman, J. T.; Manbeck, G. F.; Fujita, E. CO_2 Hydrogenation to Formate and Methanol as an Alternative to Photo- and Electrochemical CO_2 Reduction. *Chem. Rev.* **2015**, *115*, 12936; (c) Burkart, M. D.; Hazari, N.; Tway, C. L.; Zeitler, E. L. Opportunities and Challenges for Catalysis in Carbon Dioxide Utilization. *ACS Catal.* **2019**, *9*, 7937; (d) Hepburn, C.; Adlen, E.; Beddington, J.; Carter, E. A.; Fuss, S.; Mac Dowell, N.; Minx, J. C.; Smith, P.; Williams, C. K. The Technological and Economic Prospects for CO_2 Utilization and Removal. *Nature* **2019**, *575*, 87.
6. Hazari, N.; Heimann, J. E. Carbon Dioxide Insertion into Group 9 and 10 Metal-Element σ-Bonds. *Inorg. Chem.* **2017**, *56*, 13655.
7. Tanaka, R.; Yamashita, M.; Nozaki, K. Catalytic Hydrogenation of Carbon Dioxide Using Ir(III)-Pincer Complexes. *J. Am. Chem. Soc.* **2009**, *131*, 14168.
8. (a) Kang, P.; Cheng, C.; Chen, Z.; Schauer, C. K.; Meyer, T. J.; Brookhart, M. Selective Electrocatalytic Reduction of CO_2 to Formate by Water-Stable Iridium Dihydride Pincer Complexes. *J. Am. Chem. Soc.* **2012**, *134*, 5500; (b) Ahn, S.; Bielinski, E. A.; Lane, E. M.; Chen, Y.; Bernskoetter, W. H.; Hazari, N.; Palmore, G. T. R. Enhanced CO_2 Electroreduction Efficiency Through Secondary Coordination Effects on a Pincer Iridium Catalyst. *Chem. Commun.* **2015**, *51*, 5947.
9. Broggi, J.; Jurčík, V.; Songis, O.; Poater, A.; Cavallo, L.; Slawin, A. M. Z.; Cazin, C. S. J. The Isolation of [Pd{OC(O)H}(H)(NHC)(PR_3)] (NHC = N-Heterocyclic Carbene) and Its Role in Alkene and Alkyne Reductions Using Formic Acid. *J. Am. Chem. Soc.* **2013**, *135*, 4588.
10. (a) Bielinski, E. A.; Lagaditis, P. O.; Zhang, Y.; Mercado, B. Q.; Würtele, C.; Bernskoetter, W. H.; Hazari, N.; Schneider, S. Lewis Acid-Assisted Formic Acid Dehydrogenation Using a Pincer-Supported Iron Catalyst. *J. Am. Chem. Soc.* **2014**, *136*, 10234; (b) Bielinski, E. A.; Förster, M.; Zhang, Y.; Bernskoetter, W. H.; Hazari, N.; Holthausen, M. C. Base-Free Methanol Dehydrogenation Using a Pincer-Supported Iron Compound and Lewis Acid Co-Catalyst. *ACS Catal.* **2015**, *5*, 2404.
11. (a) Sullivan, B. P.; Meyer, T. J. Kinetics and Mechanism of Carbon Dioxide Insertion into a Metal-Hydride Bond. A Large Solvent Effect and an Inverse Kinetic Isotope Effect. *Organometallics* **1986**, *5*, 1500; (b) Konno, H.; Kobayashi, A.; Sakamoto, K.; Fagalde, F.; Katz, N. E.; Saitoh, H.; Ishitani, O. Synthesis and Properties of $[Ru(tpy)(4,4'\text{-}X_2bpy)H]^+$ (tpy=2,2′:6′,2″-terpyridine, bpy=2,2′-bipyridine, X = H and MeO), and Their Reactions with CO_2. *Inorg. Chim. Acta* **2000**, *299*, 155; (c) Creutz, C.; Chou, M. H. Rapid Transfer of Hydride Ion from a Ruthenium Complex to C1 Species in Water. *J. Am. Chem. Soc.* **2007**, *129*, 10108; (d) Darensbourg, D. J.; Kyran, S. J.; Yeung, A. D.; Bengali, A. A. Kinetic and Thermodynamic Investigations of CO_2 Insertion Reactions into Ru–Me and Ru–H Bonds – An Experimental and Computational Study. *Eur. J. Inorg. Chem.* **2013**, *2013*, 4024; (e) Huang, J.; Chen, J.; Gao, H.; Chen, L. Kinetic Aspects for the Reduction of CO_2 and CS_2 with Mixed-Ligand Ruthenium(II) Hydride Complexes Containing Phosphine and Bipyridine. *Inorg. Chem.* **2014**, *53*, 9570.

12. (a) Schmeier, T. J.; Hazari, N.; Incarvito, C. D.; Raskatov, J. R. Exploring the Reactions of CO_2 with PCP Supported Nickel Complexes. *Chem. Commun.* **2011**, *47*, 1824; (b) Suh, H.-W.; Schmeier, T. J.; Hazari, N.; Kemp, R. A. Experimental and Computational Studies of the Reaction of Carbon Dioxide with Pincer Supported Nickel and Palladium Hydrides. *Organometallics* **2012**, *31*, 8225.
13. (a) Musashi, Y.; Sakaki, S. Insertion of Carbon Dioxide into a Rhodium(III)–Hydride Bond: A Theoretical Study. *J. Chem. Soc., Dalton Trans.* **1998**, 577; (b) Musashi, Y.; Sakaki, S. Theoretical Study of Ruthenium-Catalyzed Hydrogenation of Carbon Dioxide into Formic Acid. Reaction Mechanism Involving a New Type of σ-Bond Metathesis. *J. Am. Chem. Soc.* **2000**, *122*, 3867; (c) Huang, K.-W.; Han, J. H.; Musgrave, C. B.; Fujita, E. Carbon Dioxide Reduction by Pincer Rhodium η^2-Dihydrogen Complexes: Hydrogen-Binding Modes and Mechanistic Studies by Density Functional Theory Calculations. *Organometallics* **2007**, *26*, 508.
14. Mayer, U.; Gutmann, V.; Gerger, W. The Acceptor Number - A Quantitative Empirical Parameter for the Electrophilic Properties of Solvents. *Monatsh. Chem.* **1975**, *106*, 1235.
15. Pavlovic, L.; Hopmann, K. H. Understanding the Influence of Lewis Acids on CO_2 Hydrogenation: The Critical Effect is on Formate Rotation. *Organometallics* **2023**, *42*, 3025.
16. Creutz, C.; Chou, M. H.; Hou, H.; Muckerman, J. T. Hydride Ion Transfer from Ruthenium(II) Complexes in Water: Kinetics and Mechanism. *Inorg. Chem.* **2010**, *49*, 9809.
17. Reichardt, C. Solvatochromic Dyes as Solvent Polarity Indicators. *Chem. Rev.* **1994**, *94*, 2319.
18. Espinosa, M. R.; Ertem, M. Z.; Barakat, M.; Bruch, Q. J.; Deziel, A. P.; Elsby, M. R.; Hasanayn, F.; Hazari, N.; Miller, A. J. M.; Pecoraro, M. V.; Smith, A.; Smith, N. E. Correlating Thermodynamic and Kinetic Hydricities of Rhenium Hydrides. *J. Am. Chem. Soc.* **2022**, *144*, 17939.
19. Elsby, M. R.; Espinosa, M. R.; Ertem, M. Z.; Deziel, A. P.; Hazari, N.; Miller, A. J. M.; Paulus, A. H.; Pecoraro, M. V. Carbon Dioxide Insertion into Rhenium Hydrides as a Probe for the Impact of Solvent on Linear Free Energy Relationships Between Thermodynamic and Kinetic Hydricity. *Organometallics* **2023**, *42*, 3005.
20. (a) Agarwal, J.; Johnson, R. P.; Li, G. Reduction of CO_2 on a Tricarbonyl Rhenium(I) Complex: Modeling a Catalytic Cycle. *J. Phys. Chem. A* **2011**, *115*, 2877; (b) Barakat, M.; Elhajj, S.; Yazji, R.; Miller, A. J. M.; Hasanayn, F. Kinetic Isotope Effects and the Mechanism of CO_2 Insertion into the Metal-Hydride Bond of fac-(bpy)Re$(CO)_3$H. *Inorg. Chem.* **2024**, *63*, 12133.
21. Jeletic, M. S.; Helm, M. L.; Hulley, E. B.; Mock, M. T.; Appel, A. M.; Linehan, J. C. A Cobalt Hydride Catalyst for the Hydrogenation of CO2: Pathways for Catalysis and Deactivation. *ACS Catalysis* **2014**, *4*, 3755.
22. National Academies of Sciences, Engineering, and Medicine. *Gaseous Carbon Waste Streams Utilization: Status and Research Needs.* The National Academies Press, Washington DC, 2019.
23. Börjesson, M.; Moragas, T.; Gallego, D.; Martin, R. Metal-Catalyzed Carboxylation of Organic (Pseudo)halides with CO_2. *ACS Catal.* **2016**, *6*, 6739.
24. (a) Darensbourg, D. J.; Rokicki, A. Reduction of Carbon Dioxide and Carbonyl Sulfide by Anionic Group VIB Metal Hydrides and Alkyls. Carbon-Hydrogen and Carbon-Carbon Bond Formation Processes and the Structure of [PNP][Cr$(CO)_5$SC(O)H]. *J. Am. Chem. Soc.* **1982**, *104*, 349; (b) Darensbourg, D. J.; Pala, M. Cation-Anion Interaction in the [Na-kryptofix-221][W$(CO)_5O_2$CH] Derivative and its Relevance in Carbon Dioxide Reduction Processes. *J. Am. Chem. Soc.* **1985**, *107*, 5687; (c) Lau, K.-C.; Petro, B. J.; Bontemps, S.; Jordan, R. F. Comparative Reactivity of Zr- and Pd-Alkyl Complexes with Carbon Dioxide. *Organometallics* **2013**, *32*, 6895; (d) Lau, K.-C.; Jordan, R. F. Reactivity of (Pyridine-Diimine)Fe Alkyl Complexes with Carbon Dioxide. *Organometallics* **2016**, *35*, 3658.
25. Johansson, R.; Jarenmark, M.; Wendt, O. F. Insertion of Carbon Dioxide into (PCP)Pd^{II}-Me Bonds. *Organometallics* **2005**, *24*, 4500.
26. (a) Jonasson, K. J.; Wendt, O. F. Synthesis and Characterization of a Family of POCOP Pincer Complexes with Nickel: Reactivity Towards CO_2 and Phenylacetylene. *Chem. Eur. J.* **2014**, *20*, 11894; (b) Mousa, A. H.; Bendix, J.; Wendt, O. F. Synthesis, Characterization, and Reactivity of PCN Pincer Nickel Complexes. *Organometallics* **2018**, *37*, 2581; (c) Mousa, A. H.; Polukeev, A. V.; Hansson, J.; Wendt, O. F. Carboxylation of the Ni–Me Bond in an Electron-Rich Unsymmetrical PCN Pincer Nickel Complex. *Organometallics* **2020**, *39*, 1553.
27. Lau, K.-C.; Petro, B. J.; Bontemps, S.; Jordan, R. F. Comparative Reactivity of Zr– and Pd–Alkyl Complexes with Carbon Dioxide. *Organometallics* **2013**, *32*, 6895.
28. (a) Diccianni, J. B.; Hu, C. T.; Diao, T. Insertion of CO_2 Mediated by a (Xantphos)NiI–Alkyl Species. *Angew. Chem. Int. Ed.* **2019**, *58*, 13865; (b) Somerville, R. J.; Odena, C.; Obst, M. F.; Hazari, N.; Hopmann, K. H.; Martin, R. Ni(I)–Alkyl Complexes Bearing Phenanthroline Ligands: Experimental Evidence for CO_2 Insertion at Ni(I) Centers. *J. Am. Chem. Soc.* **2020**, *142*, 10936.
29. Curado, N.; Maya, C.; López-Serrano, J.; Rodríguez, A. Boryl-Assisted Hydrogenolysis of a Nickel–Methyl Bond. *Chem. Commun.* **2014**, *50*, 15718.

30. Darensbourg, D. J.; Hanckel, R. K.; Bauch, C. G.; Pala, M.; Simmons, D.; White, J. N. A Kinetic Investigation of Carbon Dioxide Insertion Processes Involving Anionic Tungsten-Alkyl and -Aryl Derivatives: Effects of Carbon Dioxide Pressure, Counterions, and Ancillary Ligands. Comparisons with Migratory Carbon Monoxide Insertion Processes. *J. Am. Chem. Soc.* **1985**, *107*, 7463.
31. Suh, H.-W.; Guard, L. M.; Hazari, N. A Mechanistic Study of Allene Carboxylation with CO_2 Resulting in the Development of a Pd(II) Pincer Complex for the Catalytic Hydroboration of CO_2. *Chem. Sci.* **2014**, *5*, 3859.
32. Deziel, A. P.; Gahlawat, S.; Hazari, N.; Hopmann, K. H.; Mercado, B. Q. Comparative Study of CO_2 Insertion into Pincer Supported Palladium Alkyl and Aryl Complexes. *Chem. Sci.* **2023**, *14*, 8164.
33. (a) Huang, D.; Makhlynets, O. V.; Tan, L. L.; Lee, S. C.; Rybak-Akimova, E. V.; Holm, R. H. Fast Carbon Dioxide Fixation by 2,6-Pyridinedicarboxamidato-nickel(II)-hydroxide Complexes: Influence of Changes in Reactive Site Environment on Reaction Rates. *Inorg. Chem.* **2011**, *50*, 10070; (b) Huang, D.; Makhlynets, O. V.; Tan, L. L.; Lee, S. C.; Rybak-Akimova, E. V.; Holm, R. H. Kinetics and Mechanistic Analysis of an Extremely Rapid Carbon Dioxide Fixation Reaction. *Proc. Natl. Acad. Sci. U.S.A.* **2011**, *108*, 1222.
34. Zhang, X.; van Eldik, R. A Functional Model for Carbonic Anhydrase: Thermodynamic and Kinetic Study of a Tetraazacyclododecane Complex of Zinc(II). *Inorg. Chem.* **1995**, *34*, 5606.
35. Wang, H.; Xin, Z.; Li, Y. Synthesis of Ureas from CO_2. *Top. Curr. Chem.* **2017**, *375*, 49.
36. Schmeier, T. J.; Nova, A.; Hazari, N.; Maseras, F. Synthesis of PCP Supported Nickel Complexes and their Reactivity with Carbon Dioxide. *Chem. Eur. J.* **2012**, *18*, 6915.
37. Heimann, J. E.; Bernskoetter, W. H.; Guthrie, J. A.; Hazari, N.; Mayer, J. M. Effect of Nucleophilicity on the Kinetics of CO_2 Insertion into Pincer-Supported Nickel Complexes. *Organometallics* **2018**, *37*, 3649.
38. Bullock, R. M. Catalytic Ionic Hydrogenations. *Chem. Eur. J.* **2004**, *10*, 2366.